Dolomite Decomposition to (Ca, Mg)O Solid Solutions: An X-Ray Diffraction Study. Part II.

G. Spinolo and U. Anselmi Tamburini
Dipartimento di chimica fisica dell'Universita' and Centro di studi per la Termodinamica ed Elettrochimica dei sistemi salini fusi e solidi del C.N.R.

Z. Naturforsch. **39a,** 981–985 (1984); received July 30, 1984

The full decomposition of dolomites with low and high iron content at low temperatures and low pressures is discussed with reference to the free energy of mixing of the ternary system Ca, Fe, Mg/O. The actual products of the primary step are a couple of rock salt structured oxides close to the spinodal compositions and with very small particle sizes. A subsequent diffusional process can produce large crystallites with equilibrium compositions, but it is effective only when either a low-iron dolomite is used as starting material or higher temperatures are employed.

Paper I of this series [1] reported on some powder X-Ray diffraction (XRD) experiments on dolomite [$CaMg(CO_3)_2$] full decomposition to calcium and magnesium oxides. It has been shown that when the reaction is carried out at low temperatures and at partial CO_2 pressures much lower than equilibrium, the actual products are (Ca, Mg)O solid solutions. These exhibit the usual rock salt structure and compositions on either side of the composition axis although remarkably different from the equilibrium values. Equilibrium (*i.e.*, almost pure oxides) can indeed be obtained at higher temperatures. It was also in inferred that the (Ca, Mg)O solutions are formed in a direct diffusionless step, and that the strained calcite phase produced in some runs is due to CaO recarbonation.

The thermodynamic basis of the above conclusions was a simplified model of the $CaO-MgO-CO_2$ ternary system [2], where CaO and MgO were described as pure different phases. In this work an improved model is discussed, which takes into account the experimental evidence of (Ca, Mg)O solid solutions. We report also information on a natural dolomite sample of different origin with a different impurity content, and we discuss the difference in behaviour on the ground of the previous analysis [1] of the dolomite decomposition mechanisms.

Experimental and Results

Apparatus and procedure were described previously [1]. The dolomite sample* is a white rock from Natividad (California) and is characterized by a much lower iron content than the Pamplona sample of the previous work [1]. After grinding and sieving, the 5–50 μm fraction was used.

Two decomposition runs (hereafter indicated as D and E, respectively) were carried out. The decomposition temperature of run D was (853 ± 1) K; the working pressure about $5 \cdot 10^{-3}$ Torr ($\sim 7 \cdot 10^{-1}$ Pa). The reaction was almost complete after 6 h and therefore a XRD pattern was taken only on the final product (pattern D-6: see Figure 1). Run E was done at (761.0 ± 0.3) K and at a maximum working pressure of 10^{-3} Torr ($\sim 1.3 \cdot 10^{-1}$ Pa). The reaction took some 120 h, thus allowing us to record six XRD patterns during decomposition and on the final products (E-0 to E-116).

In spite of the different experimental conditions, the results of both runs are very similar (see Fig. 1) and may be discussed together. It is worth mentioning here:

(i) that only lime and periclase were detected among the decomposition products, without any evidence of calcite formation.

Reprint requests to Prof. Giorgio Spinolo, Dipartimento di Chimica Fisica dell'Universita' viale Taramelli, 16, I-27100 Pavia, Italy.

* The sample was kindly supplied by Alan W. Searcy (University of California-Berkeley and Lawrence Berkeley Laboratory) and belongs to the same batch used for a combined torsion-effusion and torsion-Langmuir study [3].

0340-4811 / 84 / 1000-0981 $ 01.30/0. – Please order a reprint rather than making your own copy.

Dieses Werk wurde im Jahr 2013 vom Verlag Zeitschrift für Naturforschung in Zusammenarbeit mit der Max-Planck-Gesellschaft zur Förderung der Wissenschaften e.V. digitalisiert und unter folgender Lizenz veröffentlicht: Creative Commons Namensnennung-Keine Bearbeitung 3.0 Deutschland Lizenz.

This work has been digitalized and published in 2013 by Verlag Zeitschrift für Naturforschung in cooperation with the Max Planck Society for the Advancement of Science under a Creative Commons Attribution-NoDerivs 3.0 Germany License.

Zum 01.01.2015 ist eine Anpassung der Lizenzbedingungen (Entfall der Creative Commons Lizenzbedingung „Keine Bearbeitung") beabsichtigt, um eine Nachnutzung auch im Rahmen zukünftiger wissenschaftlicher Nutzungsformen zu ermöglichen.

On 01.01.2015 it is planned to change the License Conditions (the removal of the Creative Commons License condition "no derivative works"). This is to allow reuse in the area of future scientific usage.

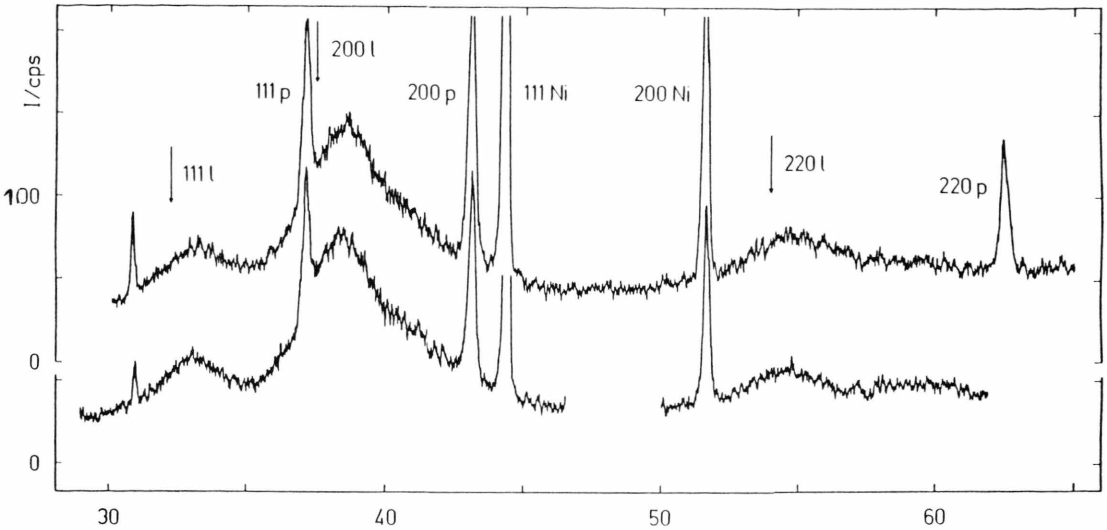

Fig. 1. Powder XRD patterns D-6 (bottom) and E-116 (top). The diffraction lines of lime (l), of periclase (p), and of the Ni specimen holder are indicated together with their crystallographic indexes.

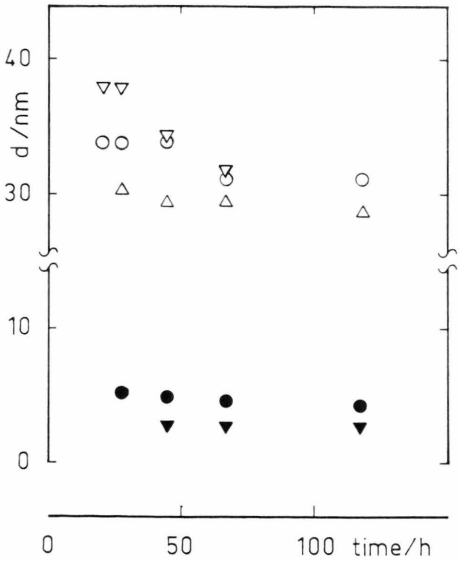

Fig. 2. Oxide particle sizes during decomposition run E, $d \sim k\lambda/[B(2\vartheta)\cos\vartheta]$, $k = 1$, $B(2\Phi)$ not corrected for instrumental broadening; circles: (111) lines; lower triangles: (200) lines; upper triangles: (220) lines; empty symbols: MgO; filled symbols: Ca-rich oxide.

(ii) that the XRD lines of lime are displaced towards high angles and remain very large during the whole reaction time (see Fig. 2), and

(iii) that the periclase lines are not significantly displaced from the expected values and their shapes indicate a much better crystallinity than lime.

Discussion

The experimental results of runs D and E are only partially in agreement with the runs (A, B and C) on high-iron dolomite [1]. Indeed, according to points (i) and (ii), the new runs show even more clearly than the former ones that lime and periclase are produced in a direct way, and that a Ca-rich (Ca, Mg)O solid solution is formed, whose small particles do not grow by diffusion over the initially formed nuclei. As in experiments A, B and C, the MgO mole fraction of this Ca-rich oxide can be evaluated in the 5 to 15% range.

On the other side, the above point (iii) looks quite surprising not only because of the disagreement, but also because it seems to indicate that the oxide products do not behave in a symmetric way. We shall discuss this argument with reference to the ternary system of calcium, iron and magnesium oxides, and, in particular, we start with a calculation of a simplified form of its phase diagram **.

** Since our interest is mainly on low temperature equilibria between rock salt structured phases, in this calculation points such as the existence of liquid or the complex behaviour of the Fe/O system are neglected: they will be taken into account only in a subsequent moment through the comparison with the experimental phase diagram, in order to correct or to straighten the conclusion of this preliminary discussion.

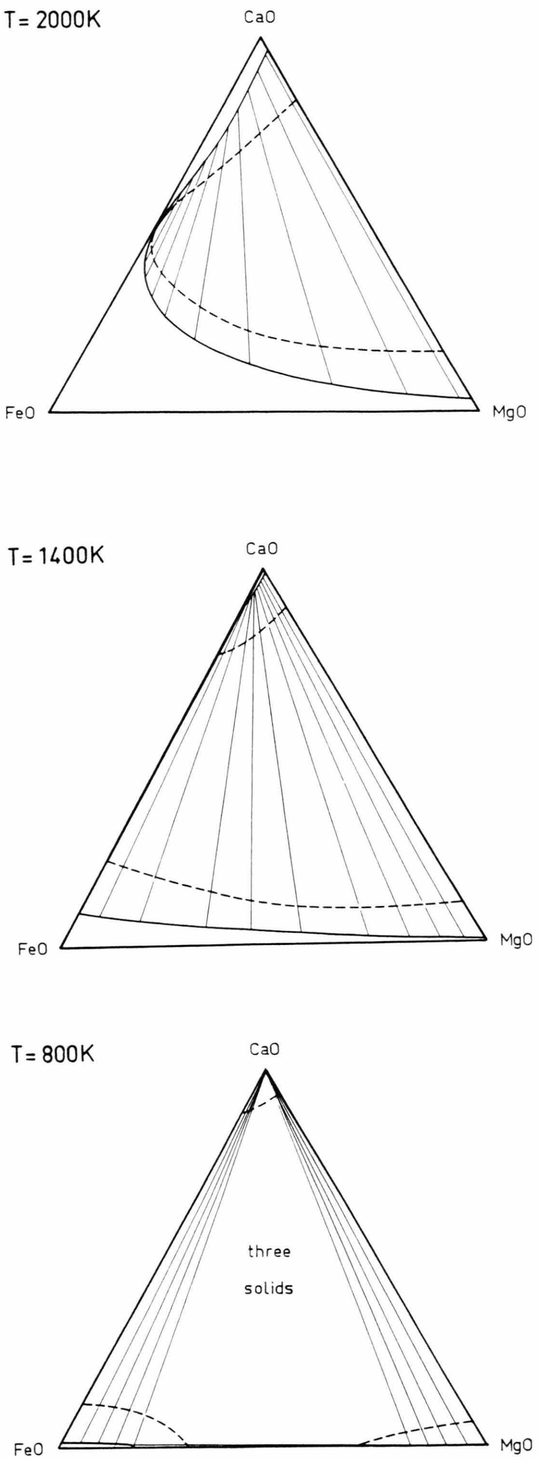

Fig. 3. Regular solution equilibria between solid phases with NaCl structure in the ternary system Ca, Fe, Mg/O: isothermal cuts at $T = 2000$ K (upper part), at $T = 1400$ K (middle part), and at 800 K (lower part).

In a comprehensive review of non-ideality in ionic systems, Davies and Navrotskyii [4] give the regular solution parameters (i.e., the so-called exchange energies) pertinent to Ca, Fe/O, Ca, Mg/O and Fe, Mg/O solid solutions ($W = 33.231$, 60.611 and 15.945 KJ mol^{-1}, respectively).

Therefore, we were able to calculate the solid state equilibria in the Ca, Fe, Mg/O ternary system by discussing the geometrical properties of the Gibbs free energy surface given by

$$G = RT \sum_{i} x_i \ln x_i + \sum_{j<k} x_j x_k W_{jk}, \tag{1}$$

where x_i is the mole fraction of component i and W_{jk} is the exchange energy for the couple of components j and k.

Figure 3 shows three isothermal sections of the ternary system: at 2000 and 1400 K (upper and middle parts, respectively) there is a large miscibility gap within the composition triangle and on the Ca, Mg/O side, and complete miscibility on the Fe, Mg/O side, whereas the Ca, Fe/O binary is either close or well below the critical point. On these diagrams, the spinodal curves (thick dashed lines) define a region where a single rock salt structured phase is intrinsically unstable and expected to undergo a spinodal decomposition; binodals (thick solid lines) and spinodals are the boundaries of metastability fields. At 800 K (lower part of the figure) the miscibility gap meets also the Fe, Mg/O side, the three monophasic fields can hardly be seen, and a triphasic field appears in the middle of the composition triangle.

This picture of the solid state equilibria is in agreement with the experimental results obtained by Johnson and Muan [5] at 1500 °C, either in air or at low oxygen pressure [$P(O_2) = 10^{-9}$ atm].

Figure 4 shows the (composition, temperature) diagram of the binary Ca, Mg/O, and the thick lines (either solid or dashed) simply show on different coordinates the regular solution results above discussed.

For the latter binary, we worked out also a more accurate free energy model to fit the available experimental data [6] (the details of the procedure are reported in the Appendix, whereas the results can be seen in Fig. 4 as thin lines, either solid or dashed). However, regardless of the model employed, a general conclusion seems to be well

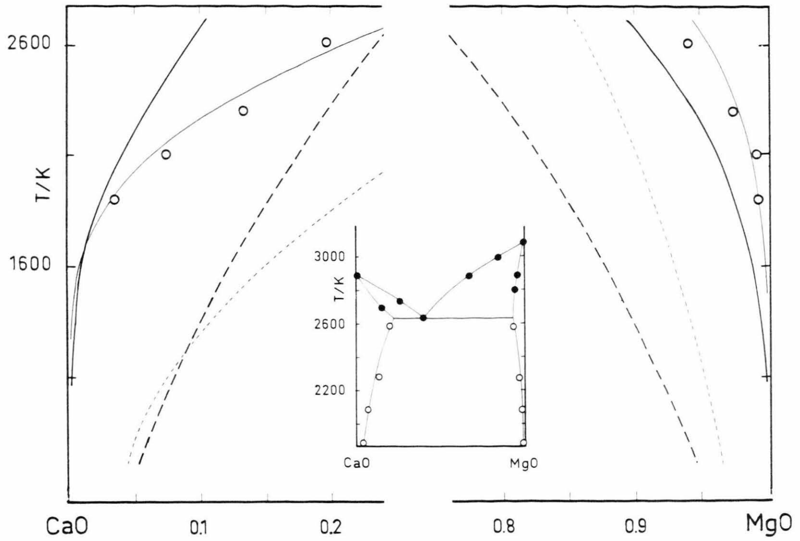

Fig. 4. Solid-solid equilibria for the binary Ca, Mg/O. Thick lines: regular solution model; thin lines: subregular model; solid lines: binodals; dashed lines: spinodals; empty circles: pertinent experimental data by Doman et al. [6]. The complete set of experimental data by the same authors is given in the insert.

established by both calculations: at the working temperatures of experiments A–E, the binodal compositions are anyway too close to the pure components to give a significant displacement of XRD line positions. Instead, the spinodal curves calculated with either model show some agreement with the non-stoichiometry of (Ca, Mg)O solutions, as it can be roughly evaluated from line shifts both on the Ca side (in all experiments) and on the Mg side (only for solutions coming from Pamplona dolomite, runs A, B and C). Although the agreement is mainly in orders of magnitude, it gives a precise meaning to an argument that was remarked in the previous paper [1], i.e., the analogy between spinodal decompositions and the direct formation of non-equilibrium (Ca, Mg)O solutions from dolomite.

Therefore the phase diagram calculation provides further support to the conclusion [1] that the primary step of dolomite full decomposition is both a chemical decomposition and a spinodal decomposition, i.e. that in the same step both a new structure is built up and the cations are splitted into two different regions as far as it is needed by stability requirements of the new structure.

In this regard, it is also worth reminding a paper by Powell and Searcy [3], who showed that in dolomite full decomposition there is an irreversible step, and that carbon dioxide desorption is not rate limiting.

The couple of (Ca, Mg)O solid solutions produced by the primary step can undergo a further step towards thermodynamic equilibrium with a diffusion controlled exchange of Ca^{++} and Mg^{++} between the different regions rich in either cation.

According to the experimental evidence the further step towards a pure CaO phase is almost always frozen, but two different results have been obtained for MgO, depending on the nature of the starting material. The low-iron Natividad sample gives almost pure periclase, whereas in the Pamplona sample the further diffusional step seems to be frozen as it is for lime. Note for instance that the periclase obtained from Natividad dolomite also displays narrow XRD peaks, thus showing that some kind of recrystallization of the primary crystallites has taken place.

Although a difference in the diffusion coefficients of Ca^{++} and Mg^{++} can reasonably justify the different results for lime and periclase coming from Natividad dolomite, we have nonetheless to explain the different behaviour of low-iron and high-iron samples. To understand a possible reason, let us come back to the Ca, Fe, Mg/O ternary system.

Looking at the calculated phase diagram, we can see that the trend of binodal and spinodal lines do not show any significant feature different from those of the Ca, Mg/O system. This is true also for FeO mole fractions much larger than the known iron content of Pamplona dolomite, so that non-stoichiometry of wüstite cannot play a significant role in this regard.

As a conclusion, the different behaviour of the two dolomite samples investigated cannot be justified on a purely thermodynamic basis by a displacement of oxide phase equilibria due to a different iron content.

However, an explaination can be tentatively given if we take into account the influence of a foreign phase on the kinetics of the diffusional step, together with the further complications due to the different iron oxidation numbers, such as reduction of carbon dioxide to produce higher valence oxides, and magnetite segregation from the non-stoichiometric field of wüstite. In this hypothesis, small amounts of magnetite, hematite or Mg-ferrite segregated at the boundaries of the primary produced crystallites can indeed slow down the diffusion controlled growth of pure MgO, which is otherwise possible at the temperatures of our experiments.

The experimental results of the present work suggest that our previous thermodynamic model [2] of dolomite system should be modified to include a (Ca, Mg)O solid solution curve. It is true that from a numerical point of view, little has to be changed, because the temperature dependence of a free energy of mixing is almost negligible with respect to that of the free energy change for alkali earth carbonates decomposition. However, a more satisfactory understanding of the full decomposition process requires a comparison of the free energy of dolomite on one side and, on the other side, the free energy of the heterogeneous mixture of carbon dioxide and of the couple of (Ca, Mg)O solutions having spinodal composition (instead of the heterogeneous mixture of carbon dioxide, pure lime and pure periclase).

Appendix

Solid State Equilibria in the Ca, Mg/O System

Solid-liquid and solid-solid equilibria for this binary system have been determined by Doman, Barr et al. [6] in the temperature range (1800–3100 K). The experimental data of solid-solid equilibria apparently show an asymmetric trend, thus suggesting that a regular solution model is not fully adequate, as it can describe only a symmetric miscibility gap.

For each experimental determination, a couple of (isothermal) connodal compositions is available, so that a free energy model with two adjustable parameters can be worked out. We did it for a subregular free energy model:

$$G = RT[x \ln x + (1-x)\ln(1-x)] + x(1-x)[A + B(1-2x)] \qquad (2)$$

(here A and B are the adjustable parameters and x is the mole fraction of MgO).

From an inspection of the resulting data, it was found that the temperature dependence of A can be empirically described by

$$A/RT = -2.37 + 1.28\,(10^4/T)\,, \qquad (3)$$

whereas for the dependence of B on temperature only one parameter is needed ($B/RT = 0.87 \pm 0.12$).

The Ca, Mg/O miscibility gap can be recalculated on the basis of the above values. The results are shown in Fig. 4 as thin lines, either solid (binodal curve) or dashed (spinodal curve). On the same figure, the thick lines correspond to the regular solution model.

Indeed, the last calculation apparently improves the quality of the fit. More significantly, by comparing the results of the different models we can see that, in either case, the solid-solid equilibria are described with a reasonable reliability even though the relevant parameters are obtained from a few experimenal data in the high temperature range.

This work was partly supported by M. P. I. (40% funds).

[1] G. Spinolo and U. Anselmi Tamburini, Z. Naturforsch. **39a,** 975 (1984).
[2] G. Spinolo and D. Beruto, J. Chem. Soc., Faraday Trans. **1, 78,** 2631 (1982).
[3] E. K. Powell and A. W. Searcy, J. Amer. Ceram. Soc. **61,** 216 (1978).
[4] P. K. Davies and A. Navrotsky, J. Solid State Chem. **46(1),** 1 (1983).
[5] E. M. Levin, C. R. Robbins, and H. F. McMurdie, Phase Diagrams for Ceramists – 1969, Supplement, The American Ceramic Society, Columbus, 1969; original measurements by R. E. Johnson and A. Muan, J. Amer. Ceram. Soc. **48,** 363 (1965).
[6] R. C. Doman, J. B. Barr, R. N. McNally, and A. M. Alper, J. Amer. Ceram. Soc. **46,** 313 (1963).